Materials and Design 46 (2013) 426–434

Contents lists available at SciVerse ScienceDirect

Materials and Design

journal homepage: www.elsevier.com/locate/matdes

Uniaxial ratcheting behavior of Zircaloy-4 tubes at room temperature

Mingjian Wen, Hua Li, Dunji Yu, Gang Chen *, Xu Chen

School of Chemical Engineering and Technology, Tianjin University, Tianjin 300072, China

ARTICLE INFO

Article history:
Received 12 September 2012
Accepted 26 October 2012
Available online 9 November 2012

Keywords:
Zirconium alloy
Cycling loading
Uniaxial ratcheting
Loading history

ABSTRACT

In this study, a series of uniaxial tensile, strain cycling and uniaxial ratcheting tests were conducted at room temperature on Zircaloy-4 (Zr-4) tubes used as nuclear fuel cladding in Pressurized Water Reactors (PWRs) for the purpose to investigate the uniaxial ratcheting behavior of Zr-4 and the factors which may influence it. The experimental results show that at room temperature this material features cyclic softening remarkably within the strain range of 1.6%, and former cycling under larger strain amplitude cannot retard cyclic softening of later cycling under lower strain amplitude. Uniaxial ratcheting strain accumulates in the direction of mean stress, and the ratcheting stain level is larger under tensile mean stress than that under compressive mean stress. Uniaxial ratcheting strain level increases with the increase of mean stress and stress amplitude, and decreases with the increase of loading rate. The sequence of loading rate appears to have no effects on the final ratcheting strain accumulation. Loading history has great influence on the uniaxial ratcheting behavior. Lower stress level after loading history with higher stress level leads to the shakedown of ratcheting. Higher loading rate after loading history with lower loading rate brings down the ratcheting strain rate. Uniaxial ratcheting behavior is sensitive to compressive pre-strain, and the decay rate of the ratcheting strain rate is slowed down by pre-compression.

1. Introduction

Zirconium alloys are widely used as structural materials for nuclear reactors because of their favorable properties like low neutron absorption cross-section [1], high corrosion resistance [2] and excellent mechanical properties [3,4] under operating conditions. Zircaloy-4 (Zr-4) is a zirconium based standard alloy, which is typically used as nuclear fuel cladding material in Pressurized Water Reactors (PWRs) [5,6]. The integrity of Zr-4 nuclear fuel cladding is very important for it not only provides an enclosure to the highly radioactive fuel but also remains in direct contact with the coolant during reactor operation [7,8].

Zr-4 nuclear fuel cladding generally undergoes uniaxial or multiaxial force damages under the combination of pressure of the external cooling medium, neutron irradiation, thermal stress and mechanical stress [9]. These forces are usually alternating. Therefore, Zr-4 nuclear fuel cladding deforms under cyclic loading conditions. In the past two decades, scholars have undertaken extensive researches to study the cyclic deformation behavior of Zr-4.

Large amount of researches go to the cyclic hardening and softening behavior. Unlike face-centered cubic (FCC) and body-centered cubic (BCC) alloys, which usually exhibit either cyclic hardening [10] or softening [11] behavior depending on the microstructure existing in the material [12,13], recrystallized Zr-4, hexagonal closed-packed (HCP) alloy, displays cyclic hardening [14,15] and also cyclic softening [16] when cycled with different total strain amplitudes and at different temperatures.

The deformation mechanisms of Zr-4 under cyclic loading are also investigated. The deformation mechanism analysis, based on the observation of the crystal structure by SEM and TEM, shows that the possible deformation modes of zirconium and its alloys include prismatic, pyramidal and basal slipping, and twinning [17,18].

By fitting the experimental data of Zr-4 under low fatigue cycle, it is reported that the low cycle fatigue life of Zr-4 follows the Coffin-Manson equation [19], and the fatigue life is affected by temperature, plasticity strain amplitude, etc. Increase of temperature leads to longer fatigue life of Zr-4 [20]. Increase of plasticity strain amplitude leads to shorter fatigue life of Zr-4 [21].

Although so many researches have been carried out to study its cyclic deformation behavior, few have been conducted under stress control with asymmetric mean stress to study the ratcheting behavior of Zr-4. Ratcheting usually leads to a shorter fatigue life of materials [22,23]. Moreover, for cyclic plastic materials, in addition to low cycle fatigue failure, the ratcheting strain accumulation reaching a threshold could also lead to failure [24]. As mentioned before, the alternating load Zr-4 nuclear fuel cladding subjected to is usually asymmetric. So, it is inevitable that the nuclear fuel

* Corresponding author. Tel.: +86 22 27408399; fax: +86 22 27403389.
E-mail address: agang@tju.edu.cn (G. Chen).

0261-3069/$ - see front matter © 2012 Elsevier Ltd. All rights reserved.
http://dx.doi.org/10.1016/j.matdes.2012.10.049

cladding will undergo ratcheting deformation. Therefore, it is essential to study the ratcheting behavior of Zr-4 in order for a comprehensive understanding of the failure mechanism of Zr-4 nuclear fuel cladding.

In this study, a series of uniaxial tensile, strain cycling and uniaxial ratcheting tests were conducted on Zr-4 tubes at room temperature. The study can not only provide guidance to a more accurate estimate of the service life of Zr-4 nuclear fuel cladding, which ensures the safety of the nuclear fuel, but also provide basic data for the establishment of the constitutive model.

2. Experiments

The chemical compositions of the Zr-4 used in this study are given in Table 1. All test specimens were tubular, with a test section of 9.5 mm outside diameter, 0.6 mm wall thickness and 100 mm length. All the specimens were tested as received, namely, without any heat treatment.

A closed-loop electro-hydraulic servo testing machine with an axial load capacity of 20 kN was used to conduct all the tests. An extensometer with a gauge length of 12.5 mm was employed to measure the axial deformation. The load, displacement, and strain were continuously monitored and recorded through the data acquisition system, and 200 data points per cycle were collected and stored for further analysis.

All the tests were conducted at room temperature. Uniaxial tensile test was carried out under strain control with strain rate of 10^{-3}/s. Strain-controlled cycling tests were conducted using a triangular waveform with strain rate of 5×10^{-3}/s. Uniaxial ratcheting tests were conducted under stress control, using triangular waveform with a combination of different loading rates, mean stresses and stress amplitudes. To further the study, a series of tests with pre-strain were also carried out. The loading conditions of uniaxial ratcheting tests without and with pre-strain are shown in Tables 2 and 3, respectively.

For the unclosed hysteresis loop of the asymmetrical stress-controlled cycling, the ratcheting strain ε_r is defined as

$$\varepsilon_r = (\varepsilon_{max} + \varepsilon_{min})/2 \quad (1)$$

where ε_{max} and ε_{min} are the maximum and minimum of axial strain in each cycle, respectively.

Table 1
The chemical compositions of Zr-4 (wt.%).

Zr	Nb	Cu	S	Ti	Hf	O	N	H
Bal.	0.90	0.013034	0.0016	0.0038	<0.01	0.11	0.002	0.001

The ratcheting strain rate $\dot{\varepsilon}_r$ is defined as

$$\dot{\varepsilon}_r = \frac{d\varepsilon_r}{dN} \quad (2)$$

where N is the number of cycles.

ε_{max}, ε_{min} and the related N can be gained directly from the data stored by the system, thus the ratcheting strain ε_r and its rate $\dot{\varepsilon}_r$ could be calculated by Eqs. (1) and (2). In this study, we define that the material reaches ratcheting shakedown status when its ratcheting strain rate $\dot{\varepsilon}_r$ is lower than 1×10^{-6}/cycle.

3. Results and discussions

In this section, the observed results on uniaxial tensile, strain cycling and uniaxial ratcheting behavior of Zr-4 tubes are given in details. The effects of mean stress, stress amplitude, loading rate and loading history on ratcheting behavior of Zr-4 are discussed. Additionally, the effects of pre-strain, mean stress direction and the sequence of loading rate on ratcheting behavior are also included in this section.

3.1. Strain-controlled tests

Stress–strain curve of uniaxial tensile test is shown in Fig. 1. From these data, linear regression is performed for the elastic part, and the obtained slope is 87 GPa, i.e. the Young's modulus of Zr-4. The curve shows continuous yielding behavior and therefore the yield strength is determined using 0.2% strain offset procedure, which is 367 MPa. Other mechanical proprieties are shown in Table 4.

Fig. 2a shows the stress–strain hysteresis loop of a three-step axial strain-controlled symmetric cycling. Each step was carried out with 200 cycles, and only the cycles of 1, 10, 30, 80, 130 and 200 are plotted. The loading history of strain amplitude was 0.5% → 0.8% → 0.5%. Fig. 2b is the corresponding stress amplitude as a function of number of cycles. It is seen that the stress amplitude decreases with the increase of the number of cycles in each step, which indicates that this material features cyclic softening within the strain range of 1.6%. This differs from the results observed by Armas et al. [12], in whose study, Zr-4 showed cyclic hardening in the initial few cycles even within the strain range of 1.4%. Moreover, former cycling under larger strain amplitude cannot retard cyclic softening behavior of later cycling under lower strain amplitude. This is different from the results observed by Yang [25] for carbon steel 45, where the material presented cyclic softening in the first two steps, but displayed cyclic hardening in step 3.

Table 2
Loading conditions of uniaxial ratcheting tests.

Specimens no.	Loading step	Stress rate (MPa/s)	Mean stress (MPa)	Stress amplitude (MPa)	Cyclic number
Zr-4#3	1	200	180	180	1000
Zr-4#4	1	200	205	230	1000
Zr-4#5	1	200	180	230	1000
	2	20	180	230	500
Zr-4#6	1	20	180	230	500
	2	200	180	230	1000
	1	200	155	230	1000
Zr-4#7	2	200	180	230	1000
	3	200	155	230	1000
	4	200	180	230	1000
	1	200	180	205	1000
Zr-4#8	2	200	180	230	1000
	3	200	180	205	1000
	4	200	180	230	1000

Table 3
Loading conditions of uniaxial ratcheting tests with compressive pre-strain.

Specimens no.	Loading step	Stress rate (MPa/s)	Mean stress (MPa)	Stress amplitude (MPa)	Pre-strain (%)	Cyclic number
Zr-4#9	1	200	180	230	–	6000
Zr-4#10	1	200	−180	230	−0.9	
	2	200	180	230	–	6000
Zr-4#11	1	200	−180	230	−1.2	
	2	200	180	230	–	6000
Zr-4#12	1	200	−180	230	−1.5	
	2	200	180	230	–	6000

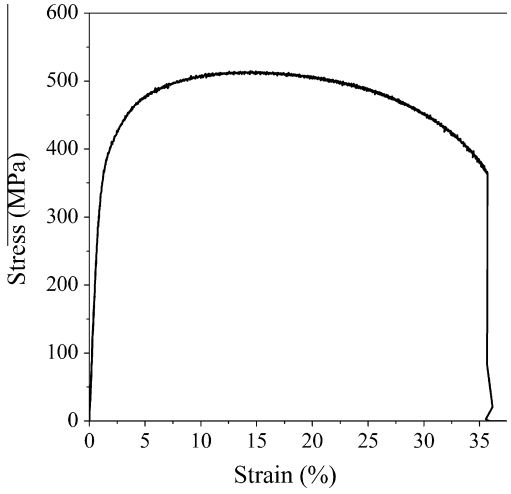

Fig. 1. Uniaxial tensile stress–strain curve.

3.2. Uniaxial ratcheting tests

Typical stress–strain hysteresis loop recorded in uniaxial ratcheting test for Zr-4 is shown in Fig. 3a, and the corresponding ratcheting strain evolution and ratcheting strain rate evolution are shown in Fig. 3b and c, respectively. The experiment was carried out about mean stress of 180 MPa, stress amplitude of 230 MPa and stress rate of 200 MPa/s. It is seen that, under asymmetric stress cycling, the initial hysteresis loop is unclose obviously. With the progress of cycling, even though this material displays unclosed hysteresis loop as well, it is not so obvious yet. The uncloseness of the hysteresis loop is the reason for the gradual ratcheting deformation of the specimen [26]. Correspondingly, the ratcheting strain accumulates rapidly in the initial state, that is, the ratcheting strain rate is high. With the increase of number of cycles, the ratcheting strain level increases, but the ratcheting strain rate decreases and tends to a stable value of 4.379×10^{-6}/cycle, which indicates that the ratcheting does not reach the shakedown status.

Strain energy density as a function of the number of cycles is plotted in Fig. 4a. In order to show the later part of the curve clearly, the partial amplification of the rectangular frame in Fig. 4a is presented in Fig. 4b. The plots show that in the initial state, strain energy density is quite large, and it reduces rapidly as the cycling progresses. At the cyclic number of about 120, it reaches the minimum value. Subsequently, it begins to increase, but the increasing rate is rather low. This phenomenon is not the same with the observation of CS1060 (also a kind of cyclic softening material) by Hassan and Kyriakides [27], in whose study, strain energy density increases monotonically.

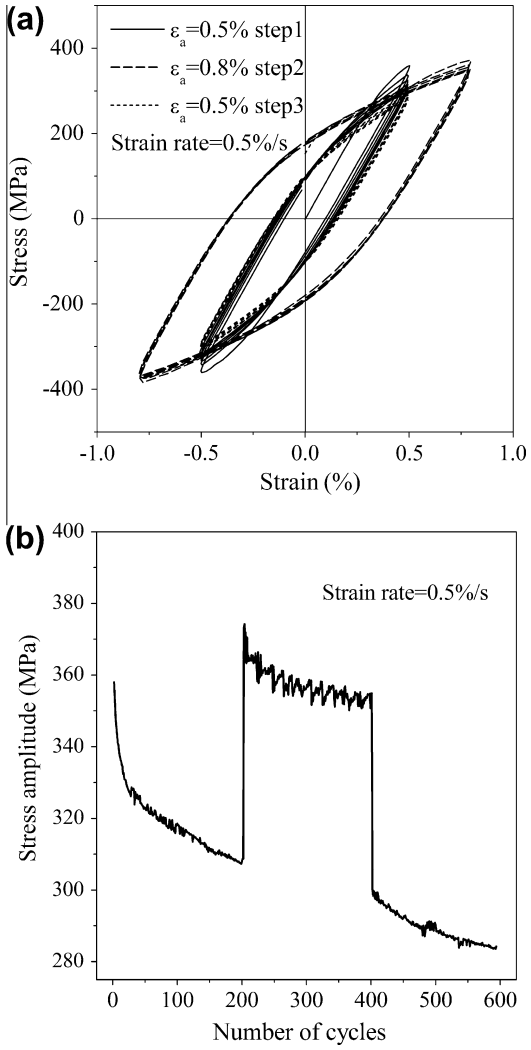

Fig. 2. Strain-controlled multistep tests: (a) stress–strain hysteresis loop; (b) stress amplitude vs. number of cycles.

Table 4
Mechanical properties of Zr-4.

Young's modulus (GPa)	Yield stress (MPa)	Ultimate tensile strength (MPa)	Uniform elongation (%)	Total elongation (%)
87	367	512	14.95	37.32

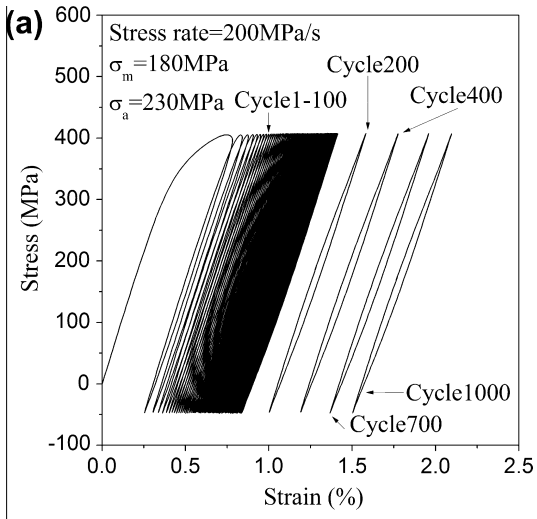

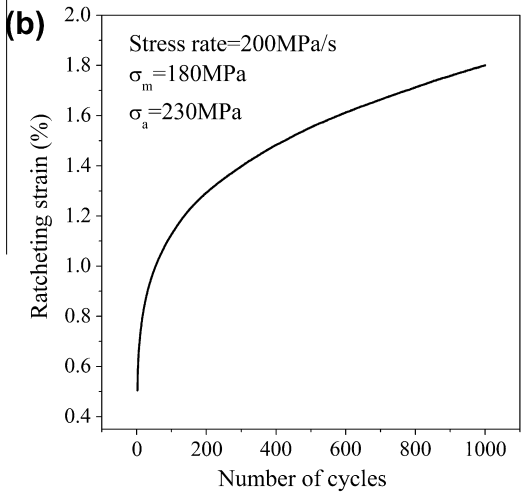

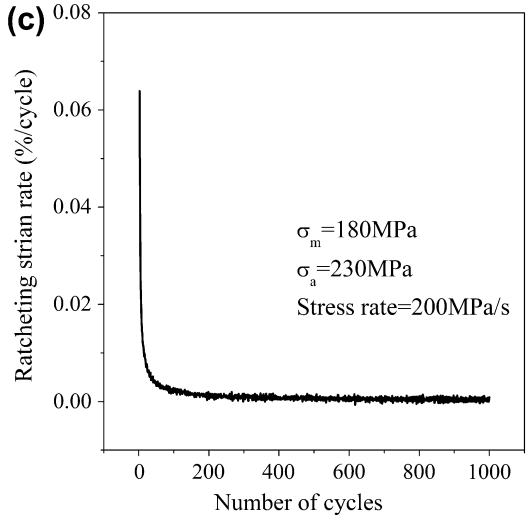

Fig. 3. Uniaxial ratcheting test: (a) stress–strain hysteresis loop; (b) ratcheting strain evolution and (c) ratcheting strain rate evolution.

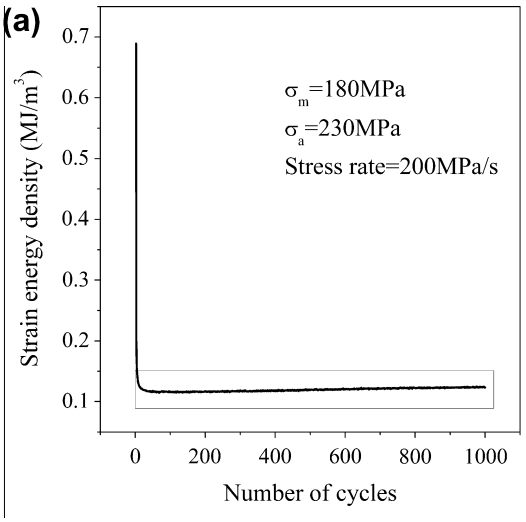

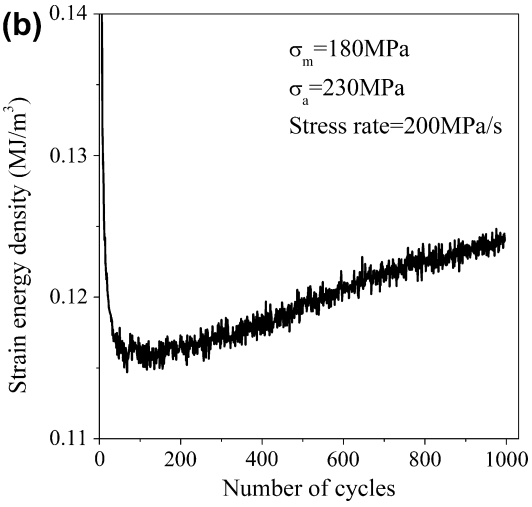

Fig. 4. Strain train energy density: (a) original; (b) partial amplification.

Two factors may affect strain energy density, one is the degree of uncloseness of the hysteresis loop and the other one is cyclic softening. As mentioned above, in the initial state, the uncloseness of the hysteresis loop is remarkable. Consequently, the area the hysteresis loop enclosing is large. With the progress of cycling, the uncloseness of the hysteresis loop becomes not so remarkable rapidly. Consequently, the enclosed area reduces rapidly. On the other hand, Zr-4 features cyclic softening, which leads to the increase of the enclosed area as the number of cycles increases. In the initial state, the decrease of the uncloseness of the hysteresis loop dominants the change of strain energy density, the decrease of strain energy density caused by which is larger than the increase of strain energy density caused by cyclic softening. Therefore, strain energy density decreases gradually in the first 120 cycles. As the cycling progresses, the discrepancy becomes smaller and smaller until the decrease of strain energy density caused by the change of the uncloseness of the hysteresis loop is smaller than the increase of strain energy density caused by cyclic softening. Then strain energy density begins to increase.

3.2.1. Effects of stress level on ratcheting behavior

Two sets of tests were conducted to investigate the way the stress level influences ratcheting behavior: one set with constant stress rate and mean stress but different stress amplitudes, and the other one with constant stress rate and stress amplitude but different mean stresses. The stress–strain hysteresis loop obtained are similar in nature to that presented in Fig. 3a, and they are not included here. Fig. 5a and b show their ratcheting strain evolution curves, respectively. It is clear from the plots that both the stress amplitude and mean stress significantly affect the ratcheting strain rate. Increase in either of them leads to a higher rate of ratcheting

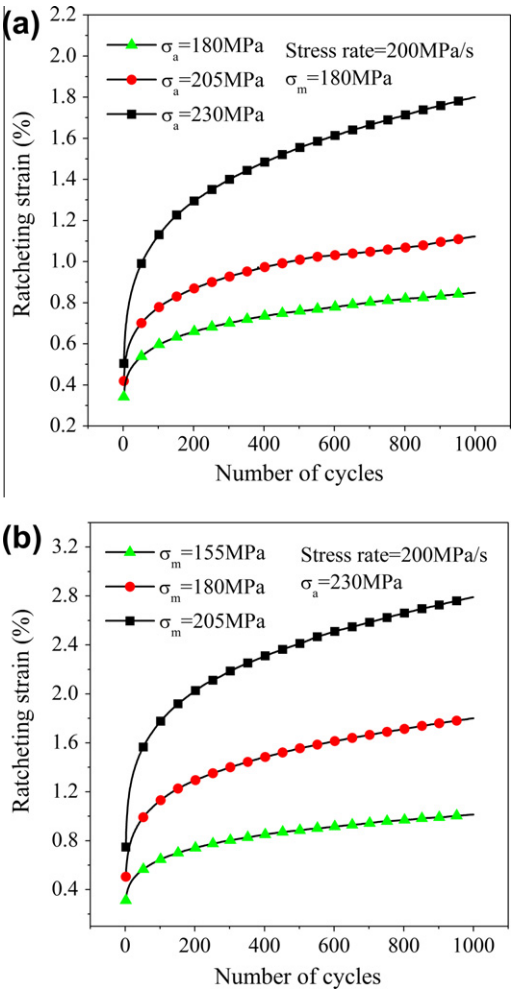

Fig. 5. Ratcheting strain evolution with: (a) constant stress rate and mean stress but different stress amplitudes; (b) constant stress rate and stress amplitude but different mean stresses.

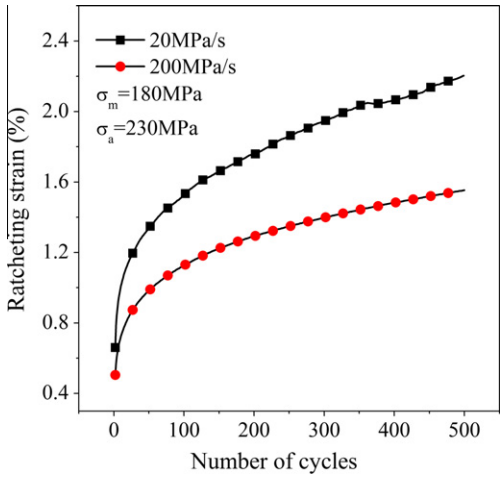

Fig. 6. Ratcheting strain evolution with constant mean stress and stress amplitude but different stress rates.

strain accumulation. This corresponds to a large amount of observation of other metals, such as CS1060 [27] and Z2CND18.12 N steel [28].

3.2.2. Effects of loading rate on ratcheting behavior

In order to investigate the effects of loading rate on ratcheting behavior, another set of tests were carried out under constant mean stress and stress amplitude but different stress rates. The ratcheting strain evolution curves are shown in Fig. 6. It is also clear that the lower the applied stress rate, the higher the ratcheting strain rate.

3.2.3. Effects of mean stress direction on ratcheting behavior

In PWRs, besides alternating loads with tensile mean values, Zr-4 nuclear fuel cladding may also undergo alternating loads with compressive mean values. Two tests were conducted to figure out the effects of mean stress direction on ratcheting behavior. Fig. 7 shows the ratcheting strain evolution curves under tensile and compressive mean stress, where, for the easiness of comparison, the mean stress of the specimen under compressive mean force is presented with absolute value. It is seen that during the whole process of ratcheting deformation, the ratcheting strain of the specimen subjected to tensile mean stress accumulates more rapidly compared with the specimen subjected to compressive mean stress. A similar phenomenon was observed for a copper alloy [29].

The reason for this phenomenon is that the tests were conducted under engineering stress control. With the progress of cycling, ratcheting deformation accumulates in the direction of mean stress. Therefore, the cross-section area of specimen under tensile mean stress decreases due to the elongation of the specimen, which causes the true stress to increase. However, the cross-section area of specimen under compressive mean stress increases because the specimen shortens, and this leads to the decrease of the true stress. As a result, during the whole process of cycling, the specimen under tensile mean stress subjects to higher stress level than the one under compressive mean stress. Consequently, the rate of ratcheting strain accumulation of the specimen under tensile mean stress is higher.

3.2.4. Effects of loading history on ratcheting behavior

In this study, multistep tests with varied mean stresses, stress amplitudes and stress rates are considered. Comparisons between specimens with and without loading history are also included.

Four-step uniaxial ratcheting test with the constant stress rate of 200 MPa/s and the constant mean stress of 180 MPa but varied stress amplitudes for each step were carried out to study the effect of history of varied stress amplitudes on ratcheting. In this case,

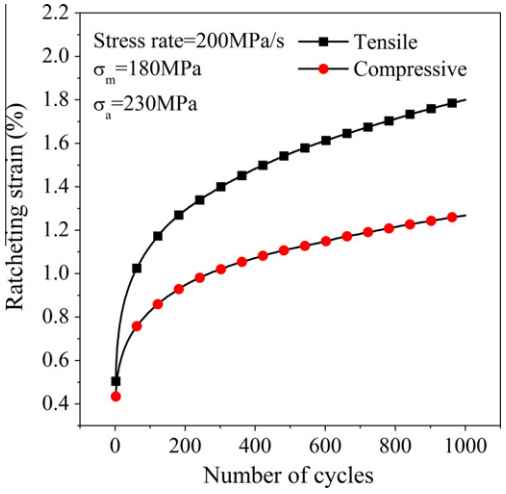

Fig. 7. Comparison of ratcheting strain evolution under tensile and compressive mean stress.

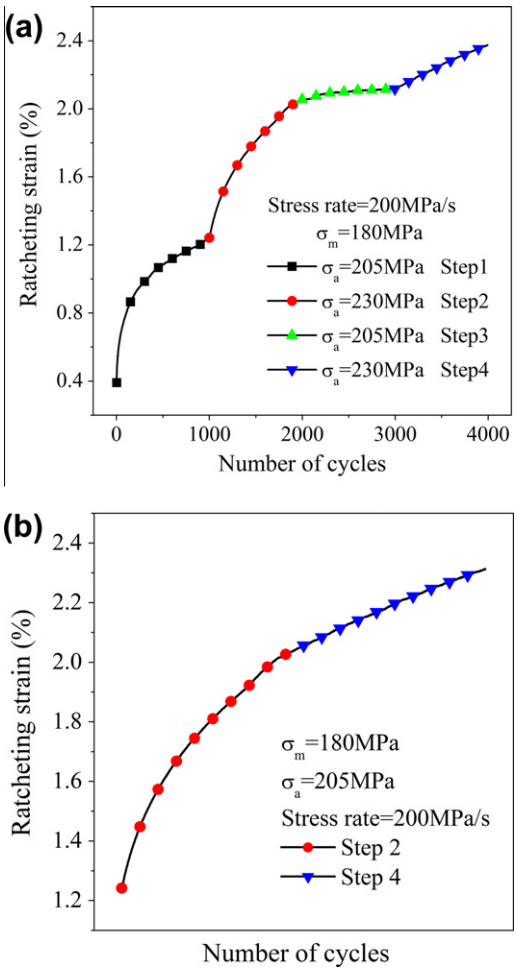

Fig. 8. Multistep test with constant stress rate and mean stress but varied stress amplitudes: (a) ratcheting strain evolution; (b) ratcheting strain evolution (step 2 and step 4).

the stress amplitudes are 205, 230, 205 and 230 MPa for step 1, 2, 3 and 4, respectively. Fig. 8a shows the ratcheting strain evolution of the multistep uniaxial ratcheting test. In step 1, the ratcheting strain rate decreases with increasing loading cycles, following a nonlinear relation with the number of cycles. Because of the increase of stress amplitude, the ratcheting strain rate in step 2 is higher than that in step 1. Step 3 witnesses nearly no ratcheting strain accumulation due to the decrease of stress amplitude. The ratcheting strain rate in step 3 gained by linear regression is 0.299×10^{-6}/cycle, smaller than 1×10^{-6}/cycle, which indicates that the ratcheting has already reached the shakedown status. The reason for this phenomenon is that the cycling under higher stress amplitude in step 2 raises the yield stress of the material; when it comes back to continue to cycle under lower stress amplitude in step 3, the peak stress only surpasses the yield stress a little, or the material even cycles in the elastic range completely, thus the ratcheting strain rate in step 3 is so low. In step 4, the stress amplitude comes back to a higher standard, which leads to faster accumulation of ratcheting strain.

The ratcheting strain in step 3 is nearly zero and the loading conditions of step 2 and step 4 are exactly the same, which leads us to refer that the ratcheting strain evolution curve of step 4 is the continuation of that of step 2. To verify this, the ratcheting strain evolution curve of step 4 is translated in such a manner that its first point coincides with the last point of the ratcheting strain curve of step 2. The result is shown in Fig. 8b. It is seen that the trends of ratcheting strain accumulation in step 2 and step 4 are almost consistent. To further verify this, the ratcheting strain rate of the last 50 cycles in step 2 and that of the first 50 cycles in step 4 are calculated through liner regression, and the ratcheting strain rates are 3.228×10^{-6}/cycle and 3.004×10^{-6}/cycle, respectively. They are rather close, so it may be safe to say the inference that the ratcheting strain evolution curve of step 4 is the continuation of that of step 2 is valid.

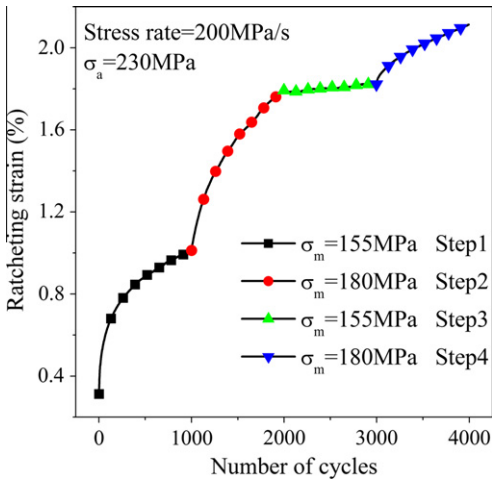

Fig. 9. Ratcheting strain evolution of multistep test with constant stress rate and stress amplitude but varied mean stresses.

Similar multistep uniaxial ratcheting test with the constant stress rate of 200 MPa/s and the constant stress amplitude of 180 MPa but varied mean stresses for each step were conducted to investigate the effect of loading history of varied mean stresses on ratcheting behavior. In this case, the mean stresses are 155, 180, 155 and 180 MPa for step 1, 2, 3 and 4, respectively. The ratcheting strain evolution curve of the four-step uniaxial ratcheting test is presented in Fig. 9.

Analysis of the plot can come to similar results with Fig. 8: loading history of cycling under higher mean stress can restrain the ratcheting strain accumulation of subsequent cycling under lower mean stress. Otherwise, the ratcheting strain continues to accumulate with a higher ratcheting strain rate. This phenomenon is in accordance with the observation of U71Mn rail steel [30], SS304 [31] and 316L stainless steel by Kang et al. [32].

From the discussion of Fig. 6, it can be seen that Zr-4 displays viscoplastic characteristic. Therefore, it is worthwhile to investigate the ratcheting behavior of Zr-4 with loading history of varied stress rates. Two two-step uniaxial ratcheting tests were conducted with the constant mean stress of 180 MPa and the constant stress amplitude of 230 MPa, and their stress rates are 200 MPa/s → 20 MPa/s and 20 MPa/s → 200 MPa/s, respectively. The ratcheting strain evolution curves are plotted in Fig. 10. The result of Fig. 10a, similar with that of specimens under loading history of varied mean stresses or stress amplitudes, is that loading history of cycling under higher stress rate cannot restrain the ratcheting strain accumulation of subsequent cycling under lower stress rate. It is seen from Fig. 10b that in step 1, the ratcheting strain rate decreases with increasing loading cycles. After 500 cycles, due to the increase of stress rate, the rate of ratcheting strain accumulation slows down and it seems to ratchet under a constant ratcheting strain rate of 1.985×10^{-6}/cycle (gained through linear regression). It is clear that the ratcheting does not reach the shakedown status.

In addition to the difference of ratcheting behavior of the same specimen under multistep loading, this section also discusses the difference of the ratcheting behavior of Zr-4 with and without loading history. The ratcheting strain evolution curves of

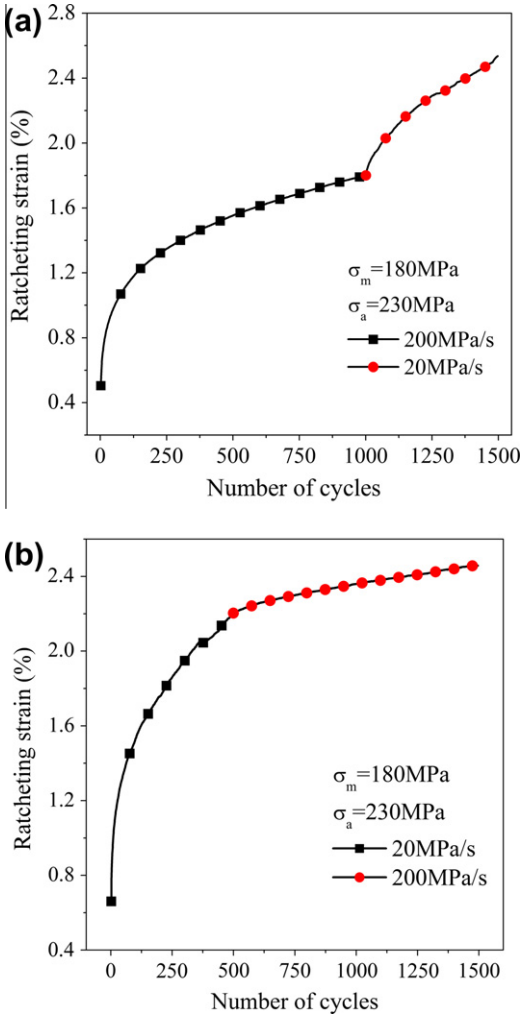

Fig. 10. Ratcheting strain evolution of multistep test with constant mean stress and stress amplitude but varied stress rates: (a) decreasing stress rate (b) increasing stress rate.

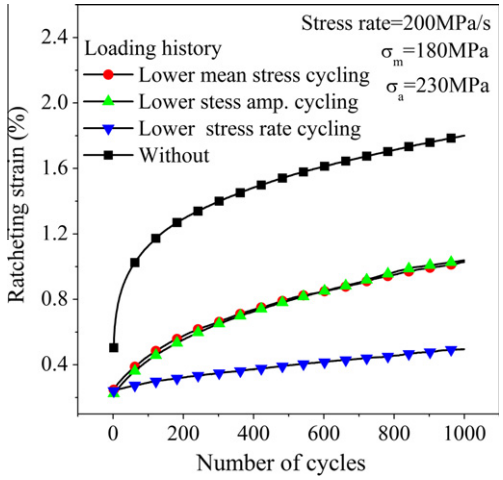

Fig. 11. Ratcheting strain evolution under the same loading condition with different loading histories (tensile).

specimens with and without loading history are shown in Fig. 11: step 1 of Zr-4#5 is the specimen without loading history; step 2 of Zr-4#7, step 2 of Zr-4#8 and step 2 of Zr-4#6 are the specimens with loading history of lower mean stress cycling, lower stress amplitude cycling and lower stress rate cycling, respectively. For specimens with loading history of lower mean stress and stress amplitude, in the initial state, the ratcheting strains accumulation are much slower than that of the specimen without loading history. Table 5 shows the ratcheting strain rates of the specimens in the stable ratcheting strain accumulation state. It is seen that their ratcheting strain rates are nearly the same with that of the specimen without loading history. The conclusion can be drawn that loading history of lower mean stress or stress amplitude only affects the ratcheting strain rate of the initial state but does not affect it in the stable ratcheting strain accumulation state. For the specimen with loading history of lower stress rate, during the whole process of cycling, the ratcheting stain rate is much lower than that of the specimen without loading history. Above all, Zr-4 is more sensitive to loading history of lower stress rate than loading history of lower mean stress or stress amplitude.

Table 5
Ratcheting strain rate of specimens with different loading histories (tensile) on the steady stage.

Specimens no.	Ratcheting strain rate (10^{-6}/cycle)
Zr-4#5 step1	4.379
Zr-4#7 step2	4.370
Zr-4#8 step2	4.560
Zr-4#6 step2	1.949

A set of tests were carried out on pre-compressed specimens under the same loading conditions with the constant stress rate of 200 MPa/s, mean stress of 180 MPa and stress amplitude of 230 MPa. The ratcheting strain evolution curves of specimens with and without pre-strain are shown in Fig. 12. Zr-4#9 is the specimen without pre-strain, and the pre-strains for step 2 of Zr-4#10, step 2 of Zr-4#11and step 2 of Zr-4#12 are 0.9%, 1.2% and 1.5%, respectively. It is clear that the strains of the specimens with pre-strain accumulate much faster than that of the specimen without pre-strain. Moreover, the larger the pre-strain is, the faster the strain accumulates. Two factors may affect the strain accumulation. One is the ratcheting strain rate and the other one is the plastic strain of the uniaxial tensile part in the first cycle. In order to figure out the dominant factor, the curves in Fig. 12a are translated in such a manner that the plastic strain of the uniaxial tensile part in the first cycle is eliminated and the ratcheting strain in the first cycle is set as 0. The result is presented in Fig. 12b. It appears that the ratcheting strain of the specimens with pre-strain accumulates slower than that of the specimen without pre-strain. Moreover, the smaller the pre-strain is, the slower the ratcheting strain accumulates. Therefore, it seems that the plastic strain of the uniaxial tensile part in the first cycle is the main factor which leads to the faster strain accumulation of pre-compressed specimens. In the stable ratcheting strain accumulation state, it is still the case that the smaller the pre-strain is, the smaller the ratcheting strain rate. However, contrary to the initial state, the ratcheting strain rates of the specimens with pre-strain are all larger than that of the specimen without pre-strain. Their ratcheting strain rates are listed in Table 6. Therefore, it may be seen that the decrease rate of the ratcheting strain rate of the specimen with pre-strain is smaller than that of the specimen without pre-strain, namely pre-compression can help to slow down the decay rate of the ratcheting strain rate.

3.2.5. Effects of sequence of loading rate on ratcheting behavior

In the former part of this paper, two groups of two-step uniaxial ratcheting tests under the constant mean stress of 200 MPa and the constant stress amplitude of 230 MPa but different loading sequence of stress rates were investigated, respectively. Here, the effects of the loading sequence on ratcheting behavior are discussed.

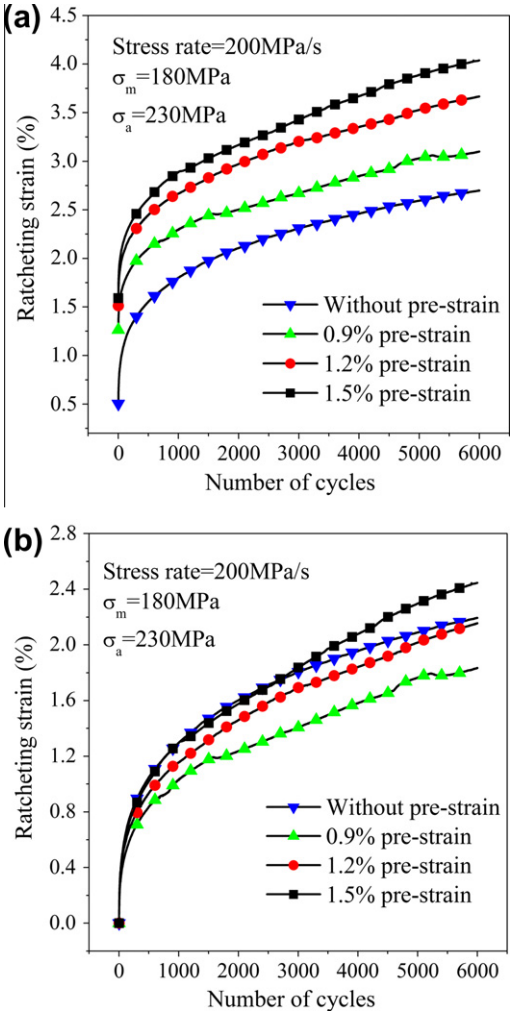

Fig. 12. Ratcheting strain evolution under the same loading condition with different loading histories (compressive): (a) original; (b) translated.

Table 6
Ratcheting strain rate of specimens with different loading histories (compressive) on the steady stage.

Specimens no.	Ratcheting strain rate (10^{-6}/cycle)
Zr-4#9	1.051
Zr-4#10 step2	1.133
Zr-4#11 step2	1.381
Zr-4#12 step2	1.508

Their ratcheting stain evolution curves are presented in Fig. 13. It shows that in the first 500 cycles, the ratcheting strain level of Zr-4#6 is much higher than that of Zr-4#5 for the reason that the stress rate of Zr-4#6 is 20 MPa/s, only 10% of that of Zr-4#5, therefore the viscosity of Zr-4 leads to the faster ratcheting strain accumulation under smaller stress rate. After cycle 500, due to the increase of the stress rate, the ratcheting strain rate of Zr-4#6 becomes smaller, and before cycle 1000, it is smaller than that of Zr-4#5. After cycle 1000, the ratcheting strain rate of Zr-4#5 becomes larger due to decrease of the stress rate. It is interesting to see that during the whole process of cycling, the ratcheting strain level of Zr-4#5 is lower than that of Zr-4#6. However, the total ratcheting strains are almost the same for both the specimens at the end, when both the specimens are cycled under the stress rate of

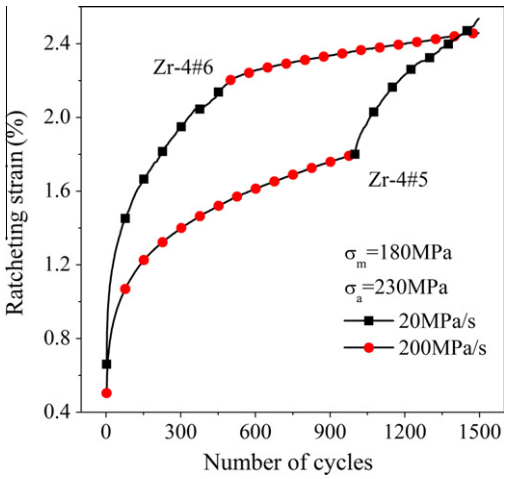

Fig. 13. Ratcheting strain evolution of multistep tests with constant mean stress and stress amplitude but different loading sequences of stress rate.

20 MPa/s for 500 cycles and 200 MPa/s for 1000 cycles. Therefore, it may be concluded that if the mean stress and stress amplitude are maintained constant, different loading rate sequence cannot affect the final ratcheting strain.

4. Conclusions

In this study, a series of uniaxial tensile, strain cycling and uniaxial ratcheting tests were conducted at room temperature on Zircaloy-4 thin-walled tubes. Based on these investigations to explore the ratcheting behavior of Zr-4 under different loading conditions, the following conclusions have been reached:

(1) Uniaxial tensile test shows that Zr-4 displays a significant strain hardening characteristics, and its Young's modulus is about 87GPa.
(2) Zr-4 features cyclic softening remarkably within the strain range of 1.6%, and former cycling under larger strain amplitude cannot retard the cyclic softening behavior of later cycling under lower strain amplitude.
(3) Uniaxial ratcheting strain of Zr-4 accumulates in the direction of mean stress. in the initial state, the ratcheting strain accumulates fast and the ratcheting strain rate is high. However, in the later part of the cycling, the ratcheting strain accumulates much slower and the ratcheting strain rate is lower correspondingly.
(4) Uniaxial ratcheting strain level of Zr-4 increases with the increase of mean stress and stress amplitude, and decreases with the increase of stress rate. Moreover, uniaxial ratcheting stain level is higher under tensile mean stress than that under compressive mean stress.
(5) Loading history has great effects on the uniaxial ratcheting behavior of Zr-4. Lower stress level after loading history with higher stress level leads to the shakedown of ratcheting. Higher loading rate after loading history with lower loading rate brings down the ratcheting strain rate. Otherwise, the ratcheting strain continues to accumulate, but the ratcheting strain level is lower compared with the specimen without loading history.
(6) Uniaxial ratcheting behavior ofZr-4 is very sensitive to compressive pre-strain, and the decay rate of the ratcheting strain rate is slowed down by pre-compression.
(7) Uniaxial ratcheting behavior of Zr-4 is affected by the sequence of loading rate, but the final ratcheting strain level

almost keeps constant for specimens cycled under different loading rate sequences.

Acknowledgements

The authors gratefully acknowledge financial support for this work from the National High Technology Research and Development Program of China (863 Program 2009AA04Z403) and Ph.D. Programs Foundation of Ministry of Education of China (No. 20090032110016).

References

[1] Lin J, Li H, Szpunar JA, Bordoni R, Olmedo AM, Villegas M, et al. Analysis of zirconium oxide formed during oxidation at 623 K on Zr–2.5Nb and Zircaloy-4. Mater Sci Eng A 2004;381:104–12.
[2] Guo D, Li M, Shi Y, Zhang Z, Zhang H, Liu X, et al. High strength and ductility in multimodal-structured Zr. Mater Des 2012;34:275–8.
[3] Mallipudi V, Valance S, Bertsch J. Meso-scale analysis of the creep behavior of hydrogenated Zircaloy-4. Mech Mater 2012;51:15–28.
[4] Lee JM, Hong SI. Design and mechanical characterization of a Zr–Nb–O–P alloy. Mater Des 2011;32:4270–7.
[5] Sridharan K, Harrington SP, Johnson AK, Licht JR, Anderson MH, Allen TR. Oxidation of plasma surface modified zirconium alloy in pressurized high temperature water. Mater Des 2007;28:1177–85.
[6] Le Saux M, Besson J, Carassou S, Poussard C, Averty X. Behavior and failure of uniformly hydrided Zircaloy-4 fuel claddings between 25 °C and 480 °C under various stress states, including RIA loading conditions. Eng Fail Anal 2010;17:683–700.
[7] Alam T, Khan MK, Pathak M, Ravi K, Singh R, Gupta SK. A review on the clad failure studies. Nucl Eng Des 2011;241:3658–77.
[8] Dunlop JW, Bréchet YJM, Legras L, Estrin Y. Dislocation density-based modelling of plastic deformation of Zircaloy-4. Mater Sci Eng A 2007;443:77–86.
[9] Xiao L, Umakoshi Y, Sun J. Biaxial low cycle fatigue properties and dislocation substructures of Zircaloy-4 under in-phase and out-of-phase loading. Mater Sci Eng A 2000;292:40–8.
[10] Li S, Hu X, Zhao Y, Lin Z, Xu N. Cyclic hardening behavior of roller hemming in the case of aluminum alloy sheets. Mater Des 2011;32:2308–16.
[11] Srivatsan TS. An investigation of the cyclic fatigue and fracture behavior of aluminum alloy 7055. Mater Des 2002;23:141–51.
[12] Armas A, Herenu S, Bolmaro R, Alvarez-Armas I. Cyclic softening mechanisms of Zircaloy-4. J Nucl Mater 2004;326:195–200.
[13] Yang C-F, Pan J-H, Lee T-H. Work-softening and anneal-hardening behaviors in fine-grained Zn–Al alloys. J Alloy Compd 2009;468:230–6.
[14] Xiao L, Gu H. Cyclic deformation behaviour and microstructure of a commercial-purity zirconium. Int J Fatigue 1994;16:417–22.
[15] Moscato MG, Avalos M, Alvarez-Armas I, Petersen C, Armas AF. Effect of strain rate on the cyclic hardening of Zircaloy-4 in the dynamic strain aging temperature range. Mater Sci Eng A 1997;234–236:834–7.
[16] Choi H, Kwun S, Lee D. Fatigue deformation mechanism of the annealed Zircaloy-4 with texture. Scripta Mater 1998;38:565–71.
[17] Xiao L, Bai JL. In situ SEM observation of monotonic and cyclic deformed structure in Zircaloy-4. Rare Metal Mater Eng 1999;28:97–100.
[18] Xiao L, Gu H. High cycle fatigue properties and microstructure of zirconium and Zircaloy-4 under reversal bending. Mater Sci Eng A 1998;252:166–73.
[19] Lee D. The role of plastic anisotropy in the fatigue behavior of Zircaloy. Metall Mater Trans B 1972;3:315–28.
[20] Xiao L, Gu H, Kuang Z. Cyclic deformation behaviour of Zircaloy-4 at different temperatures. Acta Metall Sin (Engl Lett) 1995;8:219–25.
[21] Xiao L, Gu H. Low cycle fatigue properties and microscopic deformation structure of Zircaloy-4 in recrystallized and stress-relieved conditions. J Nucl Mater 1999;265:213–7.
[22] Gao H, Chen X. Effect of axial ratcheting deformation on torsional low cycle fatigue life of lead-free solder Sn–3.5 Ag. Int J Fatigue 2009;31:276–83.
[23] Rider R, Harvey S, Chandler H. Fatigue and ratcheting interactions. Int J Fatigue 1995;17:507–11.
[24] Paul SK, Sivaprasad S, Dhar S, Tarafder S. Key issues in cyclic plastic deformation: experimentation. Mech Mater 2011;43:705–20.
[25] Yang X. Low cycle fatigue and cyclic stress ratcheting failure behavior of carbon steel 45 under uniaxial cyclic loading. Int J Fatigue 2005;27:1124–32.
[26] Mizuno M, Mima Y, Abdel-Karim M, Ohno N. Uniaxial ratchetting of 316FR steel at room temperature–Part I: Experiments. J Eng Mater Technol 2000;122:29–34.
[27] Hassan T, Kyriakides S. Ratcheting of cyclically hardening and softening materials: I. Uniaxial behavior. Int J Plasticity 1994;10:149–84.
[28] Yu D, Chen G, Yu W, Li D, Chen X. Visco-plastic constitutive modeling on Ohno–Wang kinematic hardening rule for uniaxial ratcheting behavior of Z2CND18.12N steel. Int J Plasticity 2012;28:88–101.
[29] Lim CB, Kim KS, Seong JB. Ratcheting and fatigue behavior of a copper alloy under uniaxial cyclic loading with mean stress. Int J Fatigue 2009;31:501–7.
[30] Kang G, Gao Q, Yang X. Experimental study on the cyclic deformation and plastic flow of U71Mn rail steel. Int J Mech Sci 2002;44:1647–63.
[31] Kang G, Gao Q, Cai L, Sun Y. Experimental study on uniaxial and nonproportionally multiaxial ratcheting of SS304 stainless steel at room and high temperatures. Nucl Eng Des 2002;216:13–26.
[32] Kang G, Gao Q, Cai L, Yang X, Sun Y. Experimental study on uniaxial and multiaxial strain cyclic characteristics and ratcheting of 316 L SS. C J Mater Sci Technol 2001;17:219–23.